Elastic scattering of electrons from water molecule

Liu Jun-Bo(刘俊伯)[a)b)] and Zhou Ya-Jun(周雅君)[a)†]

[a)] *Institute of Atomic and Molecular Physics, Jilin University, Changchun* 130012, *China*
[b)] *College of Physics, Beihua University, Jilin* 132001, *China*

(Received 4 October 2008; revised manuscript received 11 January 2010)

This paper uses the momentum–space optical potential method to calculate the e–H_2O scattering elastic cross sections at the energy range from 6 eV to 50 eV, and the differential cross sections in the angle from 0° to 180° at 40 eV and 50 eV. The polarisation is taken into account via an *ab initio* equivalent-local potential. The cross sections are compared with experimental measurements and other theoretical calculations.

Keywords: H_2O, the momentum-space optical potential method, elastic scattering
PACC: 3480, 3480B

1. Introduction

The study of electron collisions with the water molecule plays an important role in a wide variety of research fields, including space science, radiation physics, gas laser, planetary atmospheres and plasma etching systems.[1] The elastic scattering is fundamentally important because it is a very sensitive test for scattering theory in electron–water collision.

Various experimental measurements were used to study elastic cross sections of e–H_2O collision. Danjo and Nishimura[2] reported the first comprehensive set of absolute elastic cross section (ECS) and differential cross section (DCS) for scattering angle ranged from 15° to 120° at incident electron energies between 4 eV and 200 eV. Johnstone and Newell[3] measured the ECS and the DCS for the energy ranged from 6–50 eV and in scattering angles 10° to 120°. In the mean time, Shyn and Grafe[4] reported further cross section measurements in the energy range from 30 to 200 eV and covered higher scattering angles up to 156°. Later Cho *et al.*[5] first reported the elastic DCS for scattering angles up to 180°, and presented the ECS at incident energies between 4 and 50 eV. Recently, Itikawa and Mason[6] reported the ECS at incident energies ranged from 1 eV and 100 eV.

Several theoretical studies have also been reported on the elastic scattering of electrons from water molecules in the last two decades. The calculated DCS of H_2O for the elastic collision process were carried out by Gianturcot and Thompson[7] first for $\theta = \pi/2$. In their calculations, the single-centre model was considered by using an accurate static potential, but approximating exchange and polarisation in rather crude ways. This was improved by several other methods at different collision energies, including the static-exchange model with a parameter-free polarisation potential,[8] the single-centre expansion (SCE) approach with different models for exchange and correlation-polarisation,[9,10] the iterative Schwinger variational method plus Born closure approximation,[11] the Schwinger multichannel method with pseudopotentials (SMCPP) model,[12] and the parameter-free spherical-complex optical-potential (SCOP) model.[13] The calculations show disagreements with each other that are probably due to the different descriptions of the long-range polarisation effects among these theoretical models, and the exchange and correlation effects of higher reaction channels have not been included completely in these methods. At the scattering angle below 30° the calculated DCS values were smaller than the experimental results of Johnstone and Cho *et al.* Furthermore, the agreements of the ECS between the experimental and theoretical studies are unsatisfactory in terms of both shape and magnitude in the impact energy range from 6 eV to 50 eV. It is interesting to note that the polarisation effects play a rather crucial role in this impact energy range.

In this paper, we present new calculations by using the momentum space static-exchange-optical model.[14,15] In this method, the effects of higher reaction channels on electron–molecule elastic collisions are approximated by the *ab initio* equivalent-local po-

†Corresponding author. E-mail: yajunzhou2003@yahoo.com.cn
© 2010 Chinese Physical Society and IOP Publishing Ltd

tential, which is a complex polarisation potential: the real part of the potential describes virtual excitation of target states, which is referred as the polarisation of the target, and the imaginary part describes the real excitation of the target states, i.e. absorption. It has been applied to calculate the simplest diatomic targets like H_2, N_2 and O_2.[14−17] It is the first time that the method has been applied to calculate the elastic DCS and ECS of electron–water system.

2. Theory

The momentum space static-exchange-optical model has already been given in McCarthy and Rossi[14] and Rossi and McCarthy[15] in detail. Here we briefly review the essential features of the model employed in electron–water molecule scattering. In this case, we treat the rotation of the molecules as an adiabatic process and average over orientations of molecule. The target states are expressed in the independent-particle model by using self-consistent-field orbitals which are linear combinations of primitive Gaussians centred at the atomic sites. The wave functions of water molecules obtained by using GAMESS code. The problem is formulated in terms of a finite set of Lippmann–Schwinger integral equation for transitions between a finite discrete set of channels (in the present derivation only the elastic channel is incorporated) projected from the whole space by an operator P, which acts on the target. The remaining channels including the continuum are projected by the complementary operator Q,

$$P + Q = 1. \tag{1}$$

The P-space always includes the entrance channel, and may include other channels strongly coupled to it. Here only the former is taken into account. The momentum-space Lippmann–Schwinger equation is

$$\begin{aligned}\langle \boldsymbol{k}'0|T|0\boldsymbol{k}\rangle \;=\; & \langle \boldsymbol{k}'0|V+W|0\boldsymbol{k}\rangle \\ & +\sum_j \int d^3\boldsymbol{q}\langle \boldsymbol{k}'0|V+W|j\boldsymbol{q}\rangle \\ & \times \frac{1}{E^{(+)}-\frac{1}{2}q^2-\epsilon_j}\langle \boldsymbol{q}j|T|0\boldsymbol{k}\rangle, \end{aligned} \tag{2}$$

where $\boldsymbol{k}$ and $\boldsymbol{k}'$ are the incident and outgoing momenta of the incident electron, respectively; V represents the direct and exchange interaction potential between the electron and the target; W represents the *ab initio* equivalent local optical potential to account for polarisation effects.

As a first approximation the coupling to higher bound states j beyond the ground state can be ignored. The bound state energy eigenvalues ϵ_j include only the ground state energy ϵ_0. Then $E^{(+)} - \epsilon_j = E_0^{(+)} = \frac{1}{2}k_j^2$, where k_j is the incident electron momentum. The Green function can be rewritten in terms of the principal value denoted by P,

$$\frac{1}{E^{(+)}-\frac{1}{2}q^2-\epsilon_j} = P\frac{1}{\frac{1}{2}(k_j^2-q^2)} - \frac{\mathrm{i}\,\pi}{k_j}\delta(k_j-q). \tag{3}$$

To implement the calculation of the polarisation matrix elements $\langle \boldsymbol{k}'0|W|0\boldsymbol{k}\rangle$ we make the approximation of weak coupling of channels for which the target state is in Q-space. The time-reversed state vector for scattering with entrance channel n is denoted as $|\Psi_n^{(-)}\rangle$. Here n is a discrete notation for a one- or two-body continuum. The projection operator Q in this notation is

$$Q = \sum_n |\Psi_n^{(-)}\rangle\langle\Psi_n^{(-)}|, \tag{4}$$

and the approximation gives

$$\begin{aligned}\langle \boldsymbol{k}'0|W|0\boldsymbol{k}\rangle \;=\; & \sum_{n\in Q}\langle \boldsymbol{k}'0|V|\Psi_n^{(-)}\rangle \\ & \times \frac{1}{E^{(+)}-E_n}\langle\Psi_n^{(-)}|V|0\boldsymbol{k}\rangle. \end{aligned} \tag{5}$$

We proceed by making the Born approximation for these amplitudes. The high-energy approximation has proved excellent for optical potential matrix element in electron–atom scattering.

$$\langle\Psi_n^{(-)}(\boldsymbol{q})|V|0\boldsymbol{k}\rangle = \langle \boldsymbol{q}n|V|0\boldsymbol{k}\rangle. \tag{6}$$

Substituting Eq. (6) in Eq. (5) we obtain for the present case where P-space consists only of the ground state 0,

$$\langle \boldsymbol{k}'0|W|0\boldsymbol{k}\rangle \;=\; \int d^3\boldsymbol{q}\Big(\sum_n \langle \boldsymbol{k}'0|V|n\boldsymbol{q}\rangle \frac{1}{E^{(+)}-\varepsilon_n-\frac{1}{2}q^2}\langle \boldsymbol{q}n|V|0\boldsymbol{k}\rangle - \langle \boldsymbol{k}'0|V|0\boldsymbol{q}\rangle\frac{1}{E^{(+)}-\varepsilon_0-\frac{1}{2}q^2}\langle \boldsymbol{q}0|V|0\boldsymbol{k}\rangle. \tag{7}$$

We treat the first term of Eq. (7) by the closure approximation, which replaces ε_n by a state-independent parameter ε, and ε represents the average energy of the effectively-excited target states, thereby eliminating the target states n by the closure theorem:

$$\sum_n |n\rangle\langle n| = 1. \tag{8}$$

The parameter ε represents the average energy of the effectively-excited target states. We make one further extension to the high energy approximation by replacing ε_0 with ε in Eq. (7). This significantly simplifies the numerical analysis. It is expected to hold well in the scattering domain we are considering. The total optical potential matrix element for elastic channel scattering with incident and outgoing momenta, $\boldsymbol{k}$ and $\boldsymbol{k}'$, respectively is then

$$W(\boldsymbol{k}', \boldsymbol{k}) = W_{\rm c}(\boldsymbol{k}', \boldsymbol{k}) - W_0(\boldsymbol{k}', \boldsymbol{k}), \tag{9}$$

$$W_{\rm c}(\boldsymbol{k}', \boldsymbol{k}) = \int {\rm d}^3\boldsymbol{q} \int {\rm d}^3\boldsymbol{r} \langle \boldsymbol{k}' 0|V|\boldsymbol{r}\boldsymbol{q}\rangle \times \frac{1}{E^{(+)} - \varepsilon - \frac{1}{2}q^2} \langle \boldsymbol{q}\boldsymbol{r}|V|0\boldsymbol{k}\rangle, \tag{10}$$

$$W_0(\boldsymbol{k}', \boldsymbol{k}) = \int {\rm d}^3\boldsymbol{q} \langle \boldsymbol{k}' 0|V|0\boldsymbol{q}\rangle \times \frac{1}{E^{(+)} - \varepsilon - \frac{1}{2}q^2} \langle \boldsymbol{q}0|V|0\boldsymbol{k}\rangle. \tag{11}$$

The Green's function notation is defined with

$$G_\varepsilon^{(+)}(q) = \frac{1}{E^{(+)} - \varepsilon - \frac{1}{2}q^2}. \tag{12}$$

With closure approximation, the higher state energy eigenvalues ε_j are replaced by an average value ε. In practice the optical potential is insensitive to values of ε in a realistic range and we set ε=0. This puts the average energy at the ionisation threshold. The closure approximation is expected to be valid at incident energy several times the ionisation threshold. At such energies exchange amplitudes are relatively unimportant and are omitted. the $\boldsymbol{V}$-matrix is then evaluated,

$$\langle \boldsymbol{q}n|V|0\boldsymbol{k}\rangle = \int {\rm d}^3\boldsymbol{p} \langle \boldsymbol{r}|\boldsymbol{p}\rangle \langle \boldsymbol{q}\boldsymbol{p}|V|0\boldsymbol{k}\rangle = \frac{1}{2\pi^2|\boldsymbol{k} - \boldsymbol{q}|^2} \langle \boldsymbol{r}|0\rangle {\rm e}^{{\rm i}(\boldsymbol{k}-\boldsymbol{q})\boldsymbol{r}}, \tag{13}$$

where the ground state wave function of the molecule is represented in coordinate space by $\langle \boldsymbol{r}|0\rangle$.

Substituting Eq. (12) and the conjugate in Eq. (10), we obtain

$$W_{\rm c}(\boldsymbol{k}', \boldsymbol{k}) = \left(\int {\rm d}^3\boldsymbol{q} \frac{1}{2\pi^2|\boldsymbol{k} - \boldsymbol{q}|^2} \frac{1}{2\pi^2|\boldsymbol{k}' - \boldsymbol{q}|^2} G_\varepsilon^{(+)}(q) \right) \times \left(\int {\rm d}^3\boldsymbol{r} |\langle 0|\boldsymbol{r}\rangle|^2 {\rm e}^{{\rm i}(\boldsymbol{k}'-\boldsymbol{k})\boldsymbol{r}} \right). \tag{14}$$

Making the definition

$$\boldsymbol{P} = \boldsymbol{k}' - \boldsymbol{k} \tag{15}$$

for the momentum transfer, we have

$$W_{\rm c}(\boldsymbol{k}, \boldsymbol{P}) = \Xi(\boldsymbol{P}) \int {\rm d}^3\boldsymbol{q} \frac{1}{2\pi^2|\boldsymbol{k} - \boldsymbol{q}|^2} \frac{1}{2\pi^2|\boldsymbol{k} + \boldsymbol{P} - \boldsymbol{q}|^2} G_\varepsilon^{(+)}(q). \tag{16}$$

In the same notation, the ground state optical matrix element becomes

$$W_0(\boldsymbol{k}, \boldsymbol{P}) = \Xi(\boldsymbol{k} + \boldsymbol{P} - \boldsymbol{q}) \Xi(\boldsymbol{q} - \boldsymbol{k}) \int {\rm d}^3\boldsymbol{q} \frac{1}{2\pi^2|\boldsymbol{k} - \boldsymbol{q}|^2} \frac{1}{2\pi^2|\boldsymbol{k} + \boldsymbol{P} - \boldsymbol{q}|^2} G_\varepsilon^{(+)}(q). \tag{17}$$

Combining the two above expressions gives

$$W(\boldsymbol{k}, \boldsymbol{P}) = \int {\rm d}^3\boldsymbol{q} \frac{1}{2\pi^2|\boldsymbol{k} - \boldsymbol{q}|^2} \frac{1}{2\pi^2|\boldsymbol{k} + \boldsymbol{P} - \boldsymbol{q}|^2} G_\varepsilon^{(+)}(q) (\Xi(\boldsymbol{P}) - \Xi(\boldsymbol{k} + \boldsymbol{P} - \boldsymbol{q}) \Xi(\boldsymbol{q} - \boldsymbol{k})). \tag{18}$$

The Green's function may be reexpressed in terms of a principal value and a delta function, $E^{(+)} - \varepsilon = \frac{1}{2}k_{\rm c}^2$. For scattering below the threshold energy, the imaginary term vanishes as does the singularity at $k_{\rm c} = q$. Then the optical potential matrix element can be written as

$$W(\boldsymbol{k}, \boldsymbol{P}) = \int {\rm d}^3\boldsymbol{q} \frac{1}{2\pi^4(k_{\rm c}^2 - q^2)} \left\{ \frac{1}{|\boldsymbol{k} - \boldsymbol{q}|^2} \frac{1}{|\boldsymbol{k} + \boldsymbol{P} - \boldsymbol{q}|^2} (\Xi(\boldsymbol{P}) - \Xi(\boldsymbol{k} + \boldsymbol{P} - \boldsymbol{q}) \times \Xi(\boldsymbol{q} - \boldsymbol{k})) - \frac{1}{|\boldsymbol{k} - \boldsymbol{k}_{\rm c}|^2} \frac{1}{|\boldsymbol{k} + \boldsymbol{P} - \boldsymbol{k}_{\rm c}|^2} (\Xi(\boldsymbol{P}) - \Xi(\boldsymbol{k} + \boldsymbol{P} - \boldsymbol{k}_{\rm c}) \Xi(\boldsymbol{k}_{\rm c} - \boldsymbol{k})) \right\} - \frac{{\rm i}k_{\rm c}}{4\pi^3} \int {\rm d}\hat{q} \frac{1}{|\boldsymbol{k} - \boldsymbol{k}_{\rm c}|^2} \frac{1}{|\boldsymbol{k} + \boldsymbol{P} - \boldsymbol{k}_{\rm c}|^2} (\Xi(\boldsymbol{P}) - \Xi(\boldsymbol{k} + \boldsymbol{P} - \boldsymbol{k}_{\rm c}) \Xi(\boldsymbol{k}_{\rm c} - \boldsymbol{k})). \tag{19}$$

At this point we make a local, central approximation to the form factor in an attempt to make the calculation tractable. In the special atomic case of spherically symmetric potentials it is exact. We use the fact that

$$\int {\rm d}^3\boldsymbol{r} {\rm e}^{{\rm i}(\boldsymbol{P}\cdot\boldsymbol{r})} F(r) = G(P) \tag{20}$$

or some arbitrary local function in coordinate space, $F(r)$, to derive

$$\Xi(P) = (4\pi)^{-1} \int \mathrm{d}\hat{\boldsymbol{P}} \Xi(\boldsymbol{P}) = \int \mathrm{d}r r^2 \mathrm{j}_0(Pr) \int \mathrm{d}\hat{\boldsymbol{r}} |\langle \boldsymbol{r}|0\rangle|^2.$$

Here j_0 is the first function in the spherical Bessel function series. For future reference we name this approximation the spherical for factor approximation (SFFA). Using the molecular orbital expansions, we can write $\Xi(P)$ as

$$\begin{aligned}\Xi(P) \;=\; & 16\pi^2 \sum_{ijklml'm\sigma\xi\rho\zeta} c_{kj} c_{ij} \gamma_{kl'm'} \gamma_{ilm} (-1)^{\rho+\sigma} Y^*_{\rho\zeta}(\hat{R}_k) Y^*_{\sigma\xi}(\hat{R}_i) A^{ll'\sigma\rho}_{mm'\xi\zeta} \\ & \times \int_0^\infty \mathrm{d}r \frac{r^{l+l'+1} \sin(Pr)}{P} \exp^{-\alpha_k(r^2+R_k^2)} \exp^{-\alpha_i(r^2+R_i^2)} \mathop{\mathrm{i}}_{\sigma}(2\alpha_i r R_i) \mathop{\mathrm{i}}_{\rho}(2\alpha_k r R_k), \end{aligned} \tag{21}$$

where $\mathrm{i}_\sigma(x)$ is the spherical Bessel functions of imaginary argument; the coefficients γ transform the Cartesian representation in terms of the components x, y, z of r and x_n, y_n, z_n of the nuclear sites $\boldsymbol{R}_n$ into the spherical representation. The $A^{ll'\sigma\rho}_{mm'\xi\zeta}$ is:

$$A^{ll'\sigma\rho}_{mm'\xi\zeta} = \sum_{st} \frac{\sqrt{(2l'+1)(2\rho+1)(2\sigma+1)(2l+1)}}{4\pi(2s+1)} C^{\zeta m' t}_{\rho l' s} C^{000}_{\rho l' s} C^{\xi m t}_{\sigma l s} C^{000}_{\sigma l s}.$$

The orbital angular momentum quantum numbers l, l', m, m', ξ, ζ, σ, ρ, s, t belong to the target states i and k, respectively.

We transform our input and output channel wave vectors into vectors in the libratory frame

$$\langle \boldsymbol{k}'|T|\boldsymbol{k}\rangle = \sum_{LML'M'\mu\mu'} \langle k'L'M'||T||kLM\rangle D^L_{M\mu} D^{L'}_{M'\mu'} Y_{L'\mu'}(\hat{k}^Z) Y^*_{L'\mu'}(\hat{k}'^Z), \tag{22}$$

where the Z indicates that the wave vectors are taken in the libratory frame.

The DCS for elastic scattering can be expressed as

$$\begin{aligned}\left(\frac{\mathrm{d}\sigma}{\mathrm{d}\Omega}\right) \;=\; & (2\pi)^4 \frac{k'}{k} |\langle \boldsymbol{k}'0|T^{j0}|0\boldsymbol{k}\rangle|^2 \\ =\; & 4\pi^3 \sum_{L_1M_1L'_1M'_1\mu'_1} \sum_{L_2M_2L'_2M'_2\mu'_2} \sqrt{(2L_1+1)(2L_2+1)} \langle k'L'_1M'_1||T||kL_1M_1\rangle \langle k'L'_2M'_2||T||kL_2M_2\rangle^* \\ & \times \delta_{\mu'_1\mu'_2} \delta_{M_1+M'_2,M'_1+M_2} \sum_J \frac{1}{2J+1} C^{M_1M'_2M_1+M'_2}_{L_1L'_2J} C^{M'_1M_2M'_1+M_2}_{L'_1L_2J} C^{0\mu'_2\mu'_2}_{L_1L'_2J} Y^*_{L'_1\mu'_1}(\hat{k}'^Z) Y^*_{L'_2\mu'_2}(\hat{k}'^Z). \end{aligned} \tag{23}$$

3. Results and discussions

In the present work, we calculate the DCS for elastic scattering from H_2O at incident energies of 40 eV and 50 eV ,which are illustrated in Figs. 1 and 2. In Fig. 1, there are no other calculated results reported at this energy, the present result only compares with the experimental[2,4,5] results. At smaller angles, we found that the present DCS values are lain in the middle between the data of Shyn and Grafe[4] and Cho *et al.*[5] and the data of Danjo and Nishimura.[2] For scattering angles between 20° and 100°, the present data are in good agreement with the measurements both in the order of magnitude and in the general angular distributions. In particular the present calculated result is more close

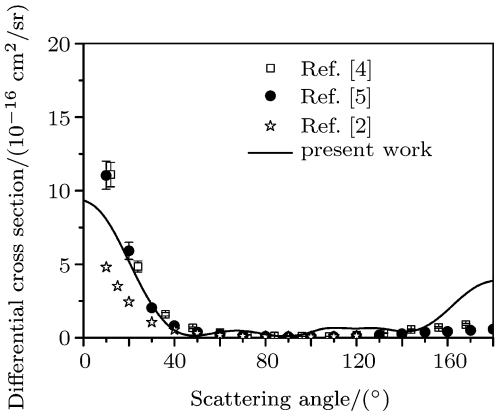


Fig. 1. The DCSs for e–H_2O scattering at 40 eV.

to the measurement of Cho *et al.*,[5] but as the angle is greater than 160°, the present results are much higher than the both measurement data. The DCS at these high angles is strongly influenced by the short-range components of the scattering potential such as the channels coupled potential. The absence of multichannel effects in the present calculation is the possible reason that cause the discrepancies between the experiments and present results.

Figure 2 shows the DCS at 50 eV along with the experimental measurements[2,3,5] and theoretical calculations.[9−11] The present result is once again lower in magnitude than the measurement data of Johnstone and Newell[3] and Cho *et al.*,[5] and higher than the data of Danjo and Nishimura as the scattering angles below 20°, which show the same trend as that in 40 eV. The present results are lower than other calculations as the scattering angles below 10°. The scattering in the forward direction is dominated by the long-range dipole interaction, which is treated by optical potential in present work.

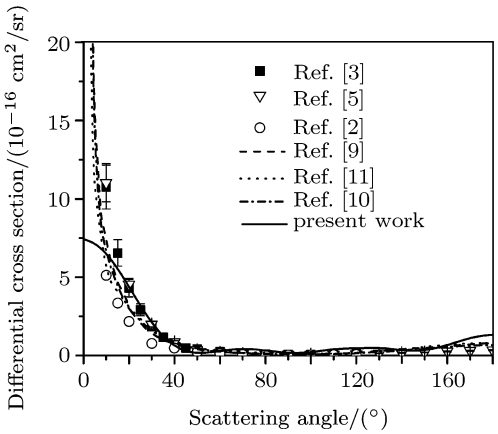


Fig. 2. The DCSs for e–H_2O scattering at 50 eV.

Okamoto *et al.*[9] have employed the Born calculation with a point-dipole potential to account for the polarisation, Gianturco *et al.*[10] included the polarisation force via a density functional approach. It is pointed out that the difference for the small-angle scattering ($\theta < 10°$) which might be attributed to the descriptions of the polarisation in these differential approaches. In scattering angles $20° < \theta < 40°$, the present curve is closer to the data obtained by Johnstone and Newell[3] and Cho *et al.*,[5] while the calculated results of Okamoto *et al.*[9] and Giantuco *et al.*[10] are lower than the experimental data of Johnstone *et al.*[3] and Cho *et al.*[5] While the scattering angle increased, the agreement between the present data and other measurements is particularly good. When the angle is greater than 160°, the result is also slightly higher than other data.

For comparison, we have calculated the ECS in 6–50 eV impact energies, which was displayed in Fig. 3,

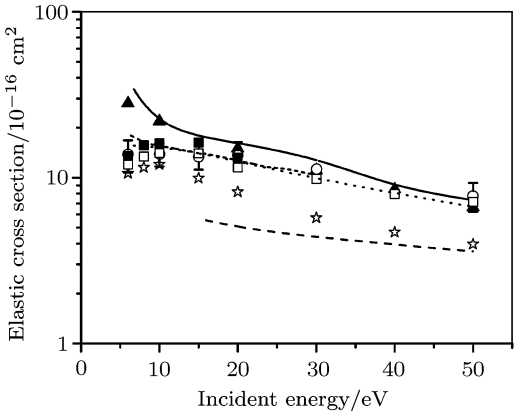


Fig. 3. The ECSs for e–H_2O scattering. Solid curve: present result; dash curve: Ref. [13]; short dash curve: Ref. [12]; Dot curve: Ref. [10]; stars: Ref. [2]; filled squares: Ref. [1]; circles with error bars: Ref. [3]; open square: Ref. [5]; filled triangles: Ref. [6].

along with experimental[2,3,5,6] data and available theoretical results. The present result is much closer to the measurement result of Itikawa and Mason[6] than all results of other calculations, which are lower than the data of Itikawa and Mason.[6] The disagreements of the measurements may be attributed to the uncertainty of each experiment in determining contributions to ECSs from forward scattering. Until recently beam experiments were unable to measure in the forward or in the backward scattering directions. Itikawa and Mason[6] succeeded in measuring with the use of a magnetic-angle-changing device. There was no available DCS that had been reported by Itikawa and Mason,[6] so we only compared their ECRs with present data. The present result is higher than the data of Shyn and Grafe[4] and Johnstone and Newell[3] particularly below 15 eV, that set the same behaviour as the calculated results of Gianturco *et al.*[10] and Vinodkumar *et al.*[13] Gianturco *et al.*[10] have included the correlation-polarisation in their SCE approach with a density function, and Vinodkumar *et al.*[13] used the SCOP method, their results are in good agreement with the data obtained by Johnstone and Newell[3] and Cho *et al.*[5] above 10 eV, but higher than the data below 10 eV. The calculated results of Varella *et al.*[12] used the SMCPP model are considerably smaller than all other experimental and theoretical results.

4. Conclusions

In summary, the comparison between our calculated DCS and ECS with experimental and other theoretical results is encouraging and shows the adequacy of the procedures used here for studying elastic electron–polar–molecule collisions. There are some discrepancies, especially at the backward angle in present calculation. This may be due to the error introduced by equivalent local approximation and single scattering channel in Lippmann–Schwinger equation. We plan to develop this method with the inclusion of an *ab initio* complex, nonlocal polarisation potential and multichannel scattering. We expect that this will lead to better agreement with experiment.

References

[1] Shyn T W and Cho S Y 1987 *Phys. Rev.* A **36** 5138
[2] Danjo A and Nishimura H 1985 *J. Phys. Soc. Japan* **54** 1224
[3] Johnstone W M and Newell W R 1991 *J. Phys.* B **24** 3633
[4] Shyn T W and Grafe A 1992 *Phys. Rev.* A **46** 4406
[5] Cho H, Park Y S, Tanaka H and Buckman S J 2004 *J. Phys.* B **37** 625
[6] Itikawa Y and Mason N 2005 *J. Phys. Chem. Ref. Data* **34** 1
[7] Gianturco F A and Thompson D G 1980 *J. Phys.* B **13** 613
[8] Jain A and Thompson D G 1982 *J. Phys.* B **15** L631
[9] Okamoto Y, Onda K and Itikawa Y 1993 *J. Phys.* B **26** 745
[10] Gianturco F A, Meloni S, Paioletti P, Lucchese R R and Sanna N 1998 *J. Chem. Phys.* **108** 4002
[11] Machado L E, Li M T, Brescansin L M, Lima M A P and Mckoy V 1995 *J. Phys.* B **28** 467
[12] Varella M T do N, Bettega M H F, Lima M A P and Ferreira L G 1999 *J. Chem. Phys.* **111** 6396
[13] Vinodkumar M, Joshipura K N, Limbachiya C and Mason N 2006 *Phys. Rev.* A **74** 022721
[14] McCarthy I E and Rossi A M 1994 *Phys. Rev.* A **49** 4645
[15] Rossi A M and McCarthy I E 1995 *J. Phys.* B **28** 3593
[16] Liu W W, Zhou Y J and Wang Z G 2003 *Chin. Phys. Lett.* **20** 1944
[17] Zheng Z, Chi B Q and Zhou Y J 2006 *Chin. Phys. Lett.* **23** 1169